Reactivity of Gas-Phase Benzene and Naphthalene Radical Cations with *N*-Methylimidazole, a Model DNA Base

Andy B. Whitehill, M. George, and Michael L. Gross*

Contribution from the Departments of Chemistry, Washington University, St. Louis, Missouri 63130, and University of Nebraska, Lincoln, Nebraska 68588-0304

Received July 17, 1995[⊗]

Abstract: The focus of this research is to evaluate the gas-phase reactivity of benzene and naphthalene radical cations with the model DNA base, *N*-methylimidazole, by using mass spectrometric techniques. Results show that in ionized mixtures of benzene/*N*-methylimidazole and naphthalene/*N*-methylimidazole, radical−cation adducts are produced. Through ion selection experiments with a Fourier transform mass spectrometer, it is shown that benzene neutrals and *N*-methylimidazole radical cations are the reactants, leading to a radical−cation adduct of *m*/*z* 160, whereas naphthalene radical cations and *N*-methylimidazole neutrals are the reactants leading to a radical−cation adduct of *m*/*z* 210. Further, the adducts have structures in which the polycyclic aromatic hydrocarbon (PAH) moiety is predominantly attached to the *N*-3 position of the imidazole ring. This attachment is analogous to adducts formed in solution reactions of PAH radical cations with DNA as well as those isolated from biological systems wherein one-electron oxidation of the aromatic compound is thought to be the activating step.

Introduction

Polycyclic aromatic hydrocarbons (PAHs) are one of the largest classes of known exogenous carcinogens. Owing to the large number of PAHs, to their ability to facilitate tumor formation, and to their ubiquitous presence in the environment, the attempt to understand PAH biological chemistry has been a large field of research.

In the mid-1990's, Miller and Miller[1] proposed that most carcinogens must first be activated to a reactive form before covalent binding to cellular nucleophiles such as DNA and eventually tumor formation can occur. Activation of PAHs is thought to occur by three different pathways. The first and most widely accepted is enzymatic oxidation and hydrolysis to form bay-region diol epoxides.[2] Most recently, benzylic electrophilic ester formation, through a series of substitution reactions, has been proposed as an activation method leading to aralkyl-DNA adduct formation.[3] A third method of activation, which has been proposed by Cavalieri and Rogan,[4] involves the creation of PAH radical cations through enzymatic one-electron oxidation. Our goal is a deeper understanding of the radical−cation activation mechanism to promote a more complete understanding of cellular carcinogenic chemistry.

PAH radical cations lead to adduct formation with cellular nucleophiles. In 1988, Rogan et al.[5] showed that adduct formation occurs between electrochemically and enzymatically generated benzo[*a*]pyrene radical cations and nucleosides. Further studies showed adduct formation to occur between benzo[*a*]pyrene radical cations and DNA as a result of reactions catalyzed by cytochrome P-450 in rat liver microsomes and nuclei.[6] 7,12-Dimethylbenz[*a*]anthracene[7] and dibenzo[*a*,*l*]-pyrene[8] also give PAH radical cations that form adducts in reaction with nucleosides. In these and a related report,[9] we showed that tandem mass spectrometry is effective in the determination of DNA adducts formed by reactions with PAH radical cations.

Although the chemistry of PAHs in a complex biological milieu is responsible for their mutagenic properties, the inherent reactivity of these species is also of interest. Inherent reactivities are established through reactions in the gas phase where there are no solvent effects. Inherent reactivities can also be modeled with molecular orbital (MO) calculations. For instance, Pross et al.[10] have published theoretical interpretations for polar reactions of radical and aryl cations with nucleophiles. They have studied "allowed" and "forbidden" reaction parameters through the use of the configuration-mixing model. The present study will provide experimental data that can be compared with results of theoretical studies.

Our purpose of this research is to build a foundation for an extensive study of relative gas-phase reactivities of a series of PAH radical cations with a common nucleophile. Because mass spectrometry can be used as a tool to generate and carry out reactions of radical cations, it was chosen for determining intrinsic reactivities of a series of PAHs. By building on this

* Present address: Washington University, Chemistry Department, One Brookings Drive, St. Louis, MO 63130.

[⊗] Abstract published in *Advance ACS Abstracts,* January 15, 1996.

(1) (a) Miller, E. C.; Miller, J. A. *Pharmacol. Rev.* **1966**, *18*, 805. (b) Miller, J. A. *Cancer Res.* **1970**, *30*, 554.

(2) (a) Sims, P.; Grover, P. L.; Swaisland, A.; Pal, K.; Hewer, A. *Nature* **1974**, *252*, 326. (b) Cooper, C. S.; Grover, P. L.; Sims, P. In *Progress in Drug Metabolism*; Bridges, J. W., Chasseaud, L. F., Eds.; John Wiley and Sons: New York, 1983.

(3) Stansbury, K. H.; Flesher, J. W.; Gupta, R. C. *Chem. Res. Toxicol.* **1994**, *7*, 254.

(4) (a) Cavalieri, E. L.; Rogan, E. G. *Free Radicals in Biology*; Academic: New York, 1984. (b) Cavalieri, E. L.; Rogan, E. G. In *Polycyclic Hydrocarbons and Carcinogenesis*; Harvey, R. G., Ed.; ACS Symposium Series 283; American Chemical Society: Washington, DC, 1985.

(5) Rogan, E. G.; Cavalieri, E. L.; Tibbels, S. R.; Cremonesi, P.; Warner, C. D.; Nagel, D. L.; Tomer, K. B.; Cerny, R. L.; Gross, M. L. *J. Am. Chem, Soc.* **1988**, *110*, 4023.

(6) Cavalieri, E. L.; Rogan, E. G.; Devanesan, P. D.; Cremonesi, P.; Cerny, R. L.; Gross, M. L.; Bodell, W. J. *Biochemistry* **1990**, *29*, 4820.

(7) RamaKrishna, N. V. S.; Cavalieri, E. L.; Rogan, E. G.; Dolnikowski, G.; Cerny, R. L.; Gross, M. L.; Jeong, H.; Jankowiak, R.; Small, G. J. *J. Am. Chem. Soc.* **1992**, *114*, 1863.

(8) RamaKrishna, N. V. S.; Padmavathi, N. S.; Cavalieri, E. L.; Rogan, E. G.; Ceryy, R. L.; Gross, M. L. *Chem. Res. Toxicol.* **1993**, *6*, 554.

(9) RamaKrishna, N. V. S.; Gao, F.; Padmavathi, N. S.; Cavalieri, E. L.; Rogan, E. G.; Cerny, R. L.; Gross, M. L. *Chem. Res. Toxicol.* **1992**, *5*, 293.

(10) (a) Pross, A. *J. Am. Chem. Soc.* **1986**, *108*, 3537. (b) Pross, A.; Moss, R. A. *Tetrahedron Lett.* **1990**, *31*, 4553.

(11) Freeman, J. A.; Johnson, J. V.; Yost, R. A.; Kuehl, D. W. *Anal. Chem.* **1994**, *66*, 1902.

0002-7863/96/1518-0853$12.00/0

foundation study, we wish ultimately to answer the question: do gas-phase reactivities of PAH radical cations correlate with biological activities? This is a complex endeavor and will require many steps in a research plan.

Reactions of radical cations and neutral molecules can be viewed as electrophile/nucleophile reactions. Benzene and naphthalene were chosen to establish whether their radical cations are reactive, and to prepare a foundation for further work with more complex PAHs such as benzo[*a*]pyrene. *N*-Methylimidazole was chosen as a neutral for its nucleophilicity, which stems from both its aromatic character and the nonbonding electron pair localized on nitrogen. Furthermore, *N*-methylimidazole is a fairly complex nucleophile having pyridine and pyrrole-type nitrogens, a reactive aromatic carbon, and a sterically hindering methyl group. These structural attributes should render *N*-methylimidazole useful in distinguishing the gas-phase reactivities of benzene and PAH radical cations. Another important reason is *N*-methylimidazole is volatile and can be readily used as a model for the nonvolatile purine bases of DNA. Solution reactions of PAH radical cations with guanine and adenine as well as with DNA show that PAH radical cations predominantly react with the imidazole ring of the purine bases, further justifying its choice.[5−8]

In work analogous in intent to that of the approach that we take here, Freeman et al.[11] proposed that measurements of gas-phase reactivities of radical cations with nucleophiles such as pyridine are an approach for screening complex environmental samples for biologically reactive electrophiles. Their work presents some support for the hypothesis that the inherent gas-phase reactivity of ions may serve as predictors of biological activity.

Another purpose is to study further the gas-phase bimolecular reactivity of the benzene and naphthalene. Studies involving these compounds have proven to be informative and important to basic mass spectrometry and have been pursued by a number of groups. Field, Hamlet, and Libby[12] published early reports on the formation and thermodynamic parameters of gas-phase benzene dimers. Wexler and Clow[13] also reported on both fundamental benzene radical cation chemistry and gas-phase reactivity of other small hydrocarbons. Anicich and Bowers[14] extended fundamental gas-phase benzene research by investigating collisional stabilization and energy transfer efficiencies for benzene and 1,1-difluoroethylene dimers. Jones et al.[15] reported on the existence and structure of ground and excited state benzene dimers formed in the latter case from $C_6H_6^{\bullet+}$ ions having an energy 3.5 eV above the ground state.

Bimolecular reactions involving benzene, naphthalene, and other PAH ions with various neutrals have likewise been studied for a number of years. Mahle, Cooks, and Korzeniowski[16] observed gas-phase hydroxylation of benzene, naphthalene, and other low-mass hydrocarbons. We uncovered reactions of benzene radical cations and alkyl halides as a method of forming gas-phase arenium ions.[17] With Van der Hart, Koning, and Nibbering,[18] we studied photodissociation and ion−molecule reactions of various C_6H_6 radical cations. In addition, we have shown benzene radical cations to react with 1,3-butadiene via a two-step cycloaddition process to form the gas-phase 1-methylindan radical cation.[19] The present study builds on past research on the inherent gas-phase reactivity of benzene and naphthalene radical cations and uses biological activity as the motivation for new ion-chemistry studies.

Some of the results reported in this paper were obtained by applying a Fourier transform mass spectrometric technique, the RF-only mode, for the study of gas-phase adduct ions. Conventional Fourier transform mass spectrometers require pressures in the range of 1×10^{-7} Torr for normal operation. These pressures are insufficient for cooling or stabilization, through thermal collisions, of some adducts. An FTMS event, called the RF-only mode, accomplishes collisional cooling of adduct ions without diminishing the performance of the FT instrument. Previously described[20] and used to study other gas-phase adducts,[21] the RF-only-mode utilizes a high-pressure event in conjunction with a high-amplitude RF voltage to stabilize collisionally gas-phase adducts.

Experimental Section

Materials. *N*-Methylimidazole was purchased from Sigma-Aldrich (St. Louis, MO) whereas 2-phenylimidazole, 1-phenylimidazole, CH_3I, and CD_3I were purchased from Aldrich (Milwaukee, WI). Benzene-d_6 and naphthalene-d_8 were purchased from Norell, Inc. (Landisville, NJ) and Cambridge Isotope Labs (Woburn, MA), respectively. 4-Phenylimidazole was purchased from Schweizer Hall (South Plainfield, NJ). All chemicals were used as purchased.

Standard methylation procedures were used to synthesize $CH(D)_3$ standards of 1; 2; and 4-phenylimidazole. The phenylimidazoles and 1.5 M excess $CH(D)_3I$ were dissolved in benzene and refluxed at 60 °C for 2 h. Products were then extracted and analyzed with low-resolution MS.

Instrumentation. Tandem mass spectrometry experiments were carried out on a Kratos MS-50 triple analyzer[22] mass spectrometer of EBE design equipped with a MACH3 data system. The instrument was operated at an accelerating voltage of 8 kV. The mass resolving power used to select the main beam was approximately 2500 (10% valley definition) unless otherwise stated.

MS/MS experiments were conducted by using the first two sectors (E_1B) as the first stage or MS1 for main-beam selection and using E_2 as MS2 for fragment-ion detection. Sequential collisional activation or MS/MS/MS[23] experiments were performed by fragmenting 8-keV ions in the first field-free region, selecting the desired fragment ion by lowering the E_1 electric field to $[(m_2/m_1)E_0]$ and the magnetic field strength by $[(m_2/m_1)B_0]$ and using E_2 as MS3 for metastable and collisionally activated decomposition (CAD) spectrum collection, where m_1 is the mass of the source-produced ion, m_2 is the mass of the fragment ion, and E_0 and B_0 are the electric and magnetic field strengths that would focus m_1 to ESA_2. All CAD spectra were collected after the main beam was reduced to 50% by collisions with helium.

Ion−molecule reactions were initiated in the tandem mass spectrometer by 280-eV electrons, emission current of 300 μA, at reaction chamber pressures of 0.1 to 0.2 Torr. Reaction chamber pressures were measured with a custom-built pressure probe consisting of a hollow stainless steel tube, a Teflon tip at one end, and a thermocouple gauge (Teledyne Hastings, Hampton, VA) at the other. Reagents were introduced into the chemical ionization (CI) source via an all-glass heated inlet system and a heated-solids probe.

(12) (a) Field, F. H.; Hamlet, P.; Libby, W. F. *J. Am. Chem. Soc.* **1967**, *89*, 6035. (b) Field, F. H.; Hamlet, P.; Libby, W. F. *J. Am. Chem. Soc.* **1969**, *91*, 2839.
(13) Wexler, S.; Clow, R. P. *J. Am. Chem. Soc.* **1968**, *90*, 3940.
(14) Anicich, V. G.; Bowers, M. T. *J. Am. Chem. Soc.* **1974**, *96*, 1279.
(15) Jones, E. G.; Bhattacharya, A. K.; Tiernan, T. O. *Int. J. Mass. Spectrom. Ion Processes* **1975**, *17*, 147.
(16) Mahle, N. H.; Cooks, R. G.; Korzeniowski, R. W. *Anal. Chem.* **1983**, *55*, 2272.
(17) Miller, D. L.; Gross, M. L. *J. Am. Chem. Soc.* **1983**, *105*, 3783.
(18) Van der Hart, W. J.; De Koning, L. J.; Nibbering, N. M. M.; Gross, M. L. *Int. J. Mass Spectrom. Ion Processes* **1986**, *72*, 99.
(19) Holman, R. W.; Rozeboom, M. D.; Gross, M. L.; Warner, C. D. *Tetrahedron* **1986**, *22*, 6235.
(20) Rempel, D. L.; Gross, M. L. *J. Am. Soc. Mass. Spectrom.* **1992**, *3*, 589.
(21) Yu, S. J.; Holliman, C. L.; Rempel, D. L.; Gross, M. L. *J. Am. Chem. Soc.* **1993**, *115*, 9676.
(22) Tudge, H.; Evans, S.; Crow, F. W.; Lyon, P. A.; Chess, E. K.; Gross, M. L. *Int. J. Mass Spectrom. Ion Processes* **1982**, *42*, 243.
(23) Burinsky, D. J.; Cooks, R. G.; Chess, E. K.; Gross, M. L. *Anal. Chem.* **1982**, *54*, 295.

In fast atom bombardment (FAB) experiments, 3-nitrobenzyl alcohol (3-NBA) was used as the matrix, and the bombarding particles were argon atoms.

Preheating experiments were carried out as follows. The collision cell in the first field-free region (between the source and E_1) was pressurized with helium, which causes keV collisions to occur. Ions that do not dissociate lose translational energy and experience a corresponding increase in internal energy (are preheated). Energy or β slits of E_1 were used to select the "hottest" portion of the ion beam. This ion beam, in which the relative population of ions with greater internal energy was increased, can then be focused and analyzed in the normal MS/MS mode. Alexander et al.[24] and others have used similar techniques to study internal energy uptake of ions surviving keV collisions.

Kinetic-energy-release (KER) values were obtained with the Kratos MS-50 triple analyzer described earlier. The molecular ion was accelerated at 8 kV and focused with MS1 (E_1 and B_1), and KER spectra were recorded by scanning E_2 in the MIKES mode. KER values reported are fwhh after correction for the energy spread of the main beam.

FTMS experiments were carried out with a custom-built instrument[25] equipped with a Nicolet Analytical FTMS 1000 data system. Reactions were conducted in a 2.54-cm molybdenum cubic trap mounted in the field of a Varian V-3400 magnet. A 1.2-T field strength and a 1-V trapping potential were used. Reagents were ionized by the 15-eV electron beam.

RF-only-mode experiments[20] were performed by admitting reagents into the cell in approximately equimolar mixtures ($P_t = 6 \times 10^{-8}$ Torr) and ionizing. After ionization, helium was admitted into the cell to a pressure of ca. 1×10^{-4} Torr (measured with an ion gauge for up to 2 s) via a solenoid-actuated Varian leak valve. This pulse has a controllable width of 100 ms to minutes. During the high-pressure event, an 800 V, 1.25-MHz RF potential was applied to the trapping plates, causing low-energy collisions to occur. These low-energy collisions serve to "cool" the ion of interest by transferring energy from the ion to the collision gas. Neutrals were then pumped away, and ion detection was accomplished as usual in FTMS.

Results and Discussion

Adduct Formation. The first step in examining the reactivities of ionized mixtures of benzene and *N*-methylimidazole, as well as naphthalene and *N*-methylimidazole, is to determine if an adduct forms. Adduct formation was first studied via a series of chemical ionization (CI) experiments. Mixtures of benzene/*N*-methylimidazole (approximately 1:1 molar ratio) and naphthalene/*N*-methylimidazole (approximately 1:1 molar ratio) were introduced into the CI source and ionized. In both systems, radical−cation adducts are produced at ion−source pressures between 0.05 and 0.2 Torr, and the adduct formation increases with increasing source pressure. Low resolving power CI spectra (see Figure 1) illustrate that adduct formation does occur for both systems, but because the adducts were formed from ionized mixtures, we cannot determine which ion was reacting with which neutral.

Reactant Ion Determination. Most magnet sector instruments do not have the capability to allow selection of a reactant ion from one neutral species and unambiguous reaction with another neutral. Triple quadrupole mass spectrometers have this capacity whereby Q_1 selects the precursor ion, Q_2 is used as a reaction chamber and is pressurized with the desired neutral, and Q_3 is used for product detection.[11] To establish reactants, Fourier transform mass spectrometry (FTMS) was used. Experiments in a conventional FT mass spectrometer show charge exchange as the only evidence of a reaction between the two species. This is due to the low pressure (1×10^{-7} Torr) normally employed in FTMS operation; this pressure is insufficient to provide stabilizing collisions of putative adducts. To conduct higher pressure FTMS experiments, a custom-built FT mass spectrometer equipped with a cell capable of operating momentarily in RF-only mode was used (see Experimental Section).

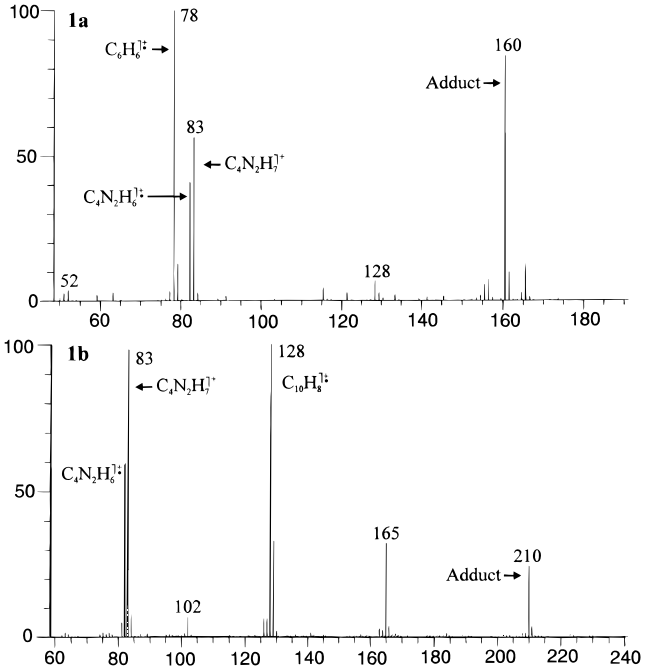

Figure 1. Low resolving mass spectra from ionized mixtures of (a) benzene/*N*-methylimidazole and (b) naphthalene/*N*-methylimidazole.

RF-only-mode experiments for the benzene/*N*-methylimidazole system showed that adduct formation occurs in the FTMS cell. Through experiments in which the benzene radical cations were selected to react with *N*-methylimidazole neutrals and vice versa, it was determined that *N*-methylimidazole radical cations and benzene neutrals are the reactants that lead to adduct formation in the FTMS cell as illustrated in eq 1.

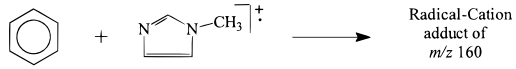

(1)

RF-only-mode experiments with the naphthalene/*N*-methylimidazole system also showed adduct formation. Through the same set of ion/neutral selection experiments, it was determined that unlike the benzene system, the naphthalene radical cation and *N*-methylimidazole neutrals are the reactants, as shown in eq 2.

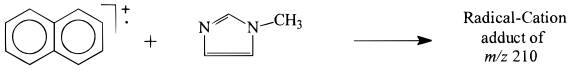

(2)

The change in the reactant ion from *N*-methylimidazole to naphthalene for the two systems is attributed to differences in ionization energies (IEs). Benzene has an IE of 9.24 eV[26] whereas that of *N*-methylimidazole is 8.66 eV.[26] Because the benzene IE is higher than that of *N*-methylimidazole, the reactivity of the benzene radical cation with neutral *N*-methylimidazole is limited to a change-exchange reaction. Naphthalene has an IE of 8.13 eV,[26] 0.53 eV lower than that of *N*-methylimidazole. In the latter system, the reactivity of the

(24) (a) Alexander, A. J.; Boyd, R. K.; Thibault, P.; Tomer, K. B. *Proc. 37th Ann. Conf. Am. Soc. Mass Spectrom.* **1989**, 226. (b) Alexander, A. J.; Thibault, P. *Rapid Commun. Mass Spectrom.* **1988**, *2*, 224.

(25) Rempel, D. L.; Gross, M. L. *J. Am. Soc. Mass. Spectrom.* **1992**, *3*, 589.

(26) Lias, S. G.; Bartmess, J. E.; Liebman, J. F.; Holmes, J. L.; Levin, R. D.; Mallard, W. G. Gas-Phase Ion and Neutral Thermochemistry. *J. Phys. Chem. Ref. Data* **1988**, *17*, Suppl. No. 1.

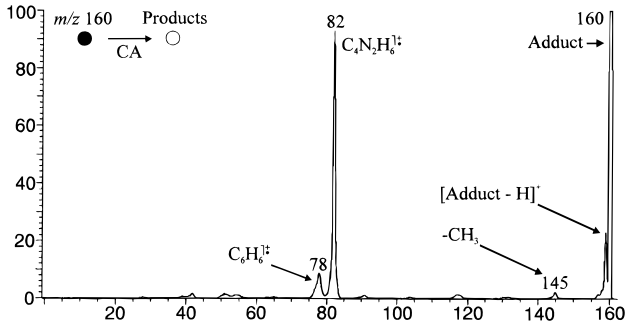

Figure 2. CAD spectrum of *m*/*z* 160 adduct produced in a mixture of ionized benzene and *N*-methylimidazole.

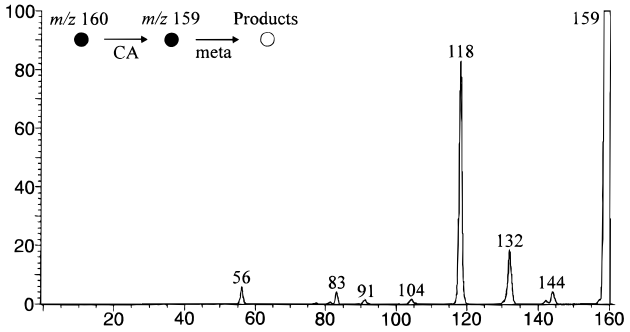

Figure 3. Metastable-induced spectrum of [adduct − H]$^+$, *m*/*z* 159. A gain factor of 200 relative to main beam intensity is applied to the product ions.

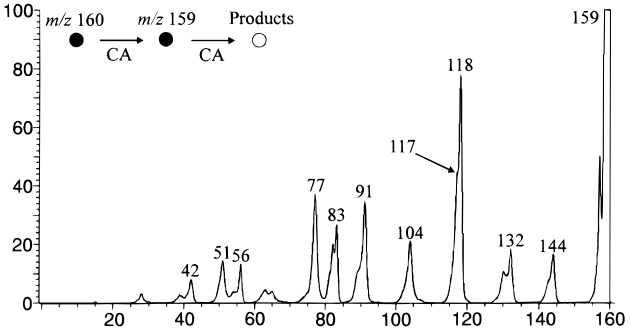

Figure 4. CAD spectrum of [adduct − H]$^+$, *m*/*z* 159. A gain factor of 75 relative to main beam intensity is applied to the product ions.

radical cation is not limited by charge exchange, and it is able to undergo adduct formation.

Adduct Structure of the Benzene System. Structural analysis of the adduct was accomplished by collecting metastable-ion and collisionally activated decomposition (CAD) spectra with the tandem sector instrument and comparing these to spectra of standards. Although eq 2 was established in a FTMS instrument, we suggest the reaction also applies to the formation of benzene/*N*-methylimidazole adducts in the CI source of the magnet sector instrument. One difference in the two experiments is the large accelerating potential used for the ionizing electrons in the sector mass spectrometer. The effective ionization energy, however, is less than the 280 eV because the high pressure in the reaction chamber moderates the electron energy. A second difference is that the number of stabilizing collisions during the rf-only-mode event can be considerably larger than in the CI source although the time between collisions is also greater.

In metastable-ion analysis, the ion of interest (i.e., the adduct ion) undergoes fragmentation without collisions, utilizing internal energy acquired during its formation. Metastable-ion spectra of the *m*/*z* 160 adduct ion show a predominant product $C_4H_6N_2$ ion of *m*/*z* 82 (presumably the *N*-methylimidazole radical cation) and a less abundant ion of *m*/*z* 78 (presumably the benzene radical cation). CAD spectra are produced by transporting the ion of interest through a collision cell pressurized with helium gas, causing high-energy collisions and subsequent fragmentations to occur. CAD spectra of the adduct show three principal fragment ions (see Figure 2): the reactant *m*/*z* 82 ion, the *m*/*z* 78 ion, and a third from loss of a hydrogen atom from the adduct. Although the metastable and CAD spectra provide little structural information, the fact that the adduct is able to produce fragment ions other than the radical cations of benzene and *N*-methylimidazole suggests that the adduct is at least in part a covalent species, although some population of loosely bound adducts cannot be ruled out.

To understand further the bonding between the benzene and *N*-methylimidazole species, kinetic-energy-release values ($T_{0.5}$) were recorded. Loosely bound species or ion−neutral complexes often exhibit $T_{0.5}$ values on the order of 10 meV or less.[27] $T_{0.5}$ values for the process of the *m*/*z* 160 adduct decomposing to form the *m*/*z* 82 (loss of 78) and *m*/*z* 78 (loss of 82) ions are 14.9 and 40.5 meV, respectively, which are inconsistent with an ion−neutral or loosely bound complex.

To probe further the structure of the adduct ion, it was decided to examine the *m*/*z* 159 ion formed by hydrogen-atom loss. The least unambiguous approach is through an MS/MS/MS experiment. The *m*/*z* 160 adduct ion was transported through a pressurized collision cell in the first field-free region of the tandem mass spectrometer, causing it to undergo hydrogen-atom loss. The resulting *m*/*z* 159 ion was then transmitted through the first ESA and the magnet sector after making appropriate adjustments to their fields and allowed to decompose metastably or activated by high-energy collisions in the third field-free region; its products were analyzed by scanning the second ESA. Figures 3 and 4 are metastable and CAD spectra, respectively, of the *m*/*z* 159 ion. Both spectra show fragment ions indicative of benzene and *N*-methylimidazole moieties.

To investigate fragmentation patterns of benzene and *N*-methylimidazole containing compounds, the standards *N*-methyl-2-phenylimidazole (**1**), *N*-methyl-4-phenylimidazole (**2**), and *N*-methyl-3-phenylimidazolium iodide (**3**) were synthesized as structural models of the [adduct − H]$^+$ ion. Compounds **1** and

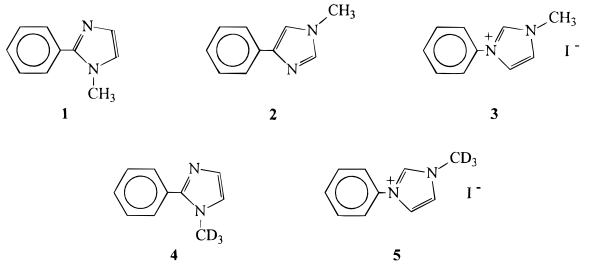

2 were synthesized as neutrals (mass 158) and require protonation and desorption by FAB to produce gas-phase ions of *m*/*z* 159 whereas the cation of **3** is a preformed quaternary ion of *m*/*z* 159 and requires desorption not ionization. Tandem mass spectra of the three standards were obtained as reference spectra after introducing the *m*/*z* 159 ions into the gas phase by protonation from the matrix if necessary, and FAB. All precursor ions show that predominant losses of 15, 27, 41, and 103 occur to form ions of *m*/*z* 144, 132, 118, and 56, respectively (see Table 1). The ions and relative abundances listed in Table

(27) (a) McAdoo, D. J. *Mass Spectrom. Rev.* **1988**, *7*, 363. (b) Holmes, J. L. *Org. Mass Spectrom.* **1985**, *20*, 169. (c) Longevialle, P. *Mass Spectrom. Rev.* **1992**, *11*, 157.

Table 1. Normalized Ion Abundances from the Metastable Decompositions of the *m*/*z* 159 Ions

product ion *m*/*z*	**1**	**2**	**3**	*m*/*z* 159 adduct
159	680000	320000	440000	24000
144	7	1	4	5
142	4		2	2
132	17	29	11	22
118	100	100	100	100
104	4		3	2
91	2	1	2	2
83				5
56	11		5	7

Table 2. Normalized Metastable-Ion Abundances of **3** at Increasing Internal Energies

product ion *m*/*z*	evacuated cell	50%[a]	70%[a]	*m*/*z* 159 adduct
144	4	4	5	5
142	2	2	2	2
132	11	15	17	22
118	100	100	100	100
104	3	3	5	2
91	2	3	5	2
83	nd[b]	nd[b]	nd[b]	5
56	5	8	9	7

[a] Percent main-beam reduction. [b] Not detected.

1 are in accord with the conclusion that the *m*/*z* 159 ion from the adduct is similar in structure to those from the standards.

Although **1**, **2**, **3**, and the adduct produce *m*/*z* 159 ions that undergo similar metastable losses, the fragment ion abundances of the *m*/*z* 159 ions from the standards are 13−30 times less than those from the $[\text{adduct} - \text{H}]^+$ ion. It is possible the *m*/*z* 159 ion from the adduct, which is created via the CAD process, has a relatively large amount of internal energy, leading to production of more abundant fragment ions. To investigate the effect of internal energy on metastable-ion losses, a preheating experiment was done to increase the internal energy of the *m*/*z* 159 ions from the standards. In this experiment, the main beam of precursor ions is allowed to undergo collisions with helium gas in the first field-free region. Some of the ions that survive intact the keV collisions will show a loss in translational energy and a corresponding increase in internal energy. These ions will appear as a "foot" on the low-energy side of the main beam and can be selected by translating the β (energy) slits of E_1 to remove the higher translational-energy (lower internal energy) ions and analyzed in the normal MS/MS mode. The metastable-ion abundances of **3** are listed in Table 2 according to internal energy, which was increased (by increasing the He pressure of collision cell #1, resulting in beam suppression and reported as such) until the yield of fragment was approximately equal to that of the adduct's *m*/*z* 159 ion. An increase in overall yield of product ions is produced by preheating and is reflected in the decrease of 15 in the gain factor used to record the ions; furthermore, the abundances of the ions of *m*/*z* 56, 91, 104, 132, and 144 increase slightly relative to that of the *m*/*z* 118 ion.

The effect of internal energy on losses induced by collisional activation was investigated by carrying out another preheating experiment. Again, the *m*/*z* 159 ion from **3** was subjected to collisions in the first field-free region to increase internal energy. Although the relative abundances of the *m*/*z* 56, 118, and 132 metastable ions increase significantly with increasing main beam internal energy, the relative abundances of CA-produced ions such as *m*/*z* 51, 77, 104, 117, 130 do not (see Table 3). This increase in the relative abundance of metastable ions during preheating is due to the fact that the population of ions that reach the third field-free region is enhanced with ions of

Table 3. Relative CAD Ion Abundances of **3** at Increasing Internal Energies

product ion *m*/*z*	evacuated cell	40%[a]	60%[a]	80%[a]
144	50	38	44	49
132	nd[b]	16	24	27
130	28	25	28	28
118	50	80	119	147
117	81	86	89	89
104	42	46	51	48
91	52	70	69	72
82	25	20	23	23
77	100	100	100	100
56	16	24	27	30
51	34	39	36	35
42	23	23	21	20
39	5	6	6	6
28	5	7	7	7

[a] Percent main-beam reduction. [b] Not detected.

Table 4. Normalized Ion Abundances[a] of Collisionally-Activated *m*/*z* 159 Ions

product ion *m*/*z*	**1**	**2**	**3**	$[\text{adduct} - \text{H}]^+$
144	93	76	50	37
130	30	47	28	25
117	92	100	81	100
104	100	41	42	46
102	nd	58	nd	nd
91	61	66	52	78
89	39	58	17	23
83	nd	nd	21	59
82	10	3	25	45
77	94	41	100	84
65	13	8	9	9
63	15	16	8	10
54	14	2	7	8
51	29	16	33	33
42	13	11	22	17
39	9	6	5	6
28	16	3	5	7

[a] The abundances of ions of *m*/*z* 56, 118, and 132 are not reported.

sufficient energy to undergo metastable losses. Without preheating the *m*/*z* 159 ions from **1**, **2**, and **3**, the relative abundances of the metastable ions of *m*/*z* 56, 118, and 132 in CAD spectra are much less abundant than those of the $[\text{adduct} - \text{H}^\bullet]$ ion. As a result, the metastable ions of *m*/*z* 56, 118, and 132 will not be considered when comparing CAD spectra of the adduct's *m*/*z* 159 ion with those of the standards.

A comparison of CAD ion abundances permits us to rule out the $[\text{M} + \text{H}]^+$ from **2** as a structure of the $[\text{adduct} - \text{H}]^+$. As shown in Table 4, the $[\text{M} + \text{H}]^+$ of **2** is identifiable and different from the $[\text{adduct} - \text{H}]^+$ ion because the former produces an abundant *m*/*z* 144 ion and a low abundance *m*/*z* 77 ion, and most importantly, it is the only species that is able to produce a *m*/*z* 102 ion (C_8H_6). The $[\text{M} + \text{H}]^+$ from **1** seems to have a different structure because it fragments to give abundant *m*/*z* 104 and 144 ions, whereas the preformed *m*/*z* 159 from **3** is most similar to the $[\text{adduct} - \text{H}]^+$ ion.

The data presented to this point suggest that the *m*/*z* 159 ion from the adduct has a structure in which C_6H_5 is attached to the imidazole ring at either or both the nitrogen-3 or the carbon-2 position. To distinguish these possibilities and to determine further the adduct structure, the methyl groups were replaced with CD_3 groups to create standards **4** and **5**. Standard **5** is a preformed cation whereas the gas-phase *m*/*z* 162 ion from **4** is produced by protonation occurring upon FAB. For comparison, benzene was reacted with *N*-(trideuteriomethyl)imidazole in the CI source and the product ion of *m*/*z* 162 produced by loss of $\text{H}^\bullet$ was analyzed with MS/MS techniques.

Comparison of CAD spectra (see Figure 5) of **4** and **5** and the corresponding *m*/*z* 162 adduct allows us to differentiate the two standards and propose a single structure for the adduct. The spectra show that nearly the same product ions are produced, but subtle differences are revealed by patterns that are made clear by the isotopic labeling. Reference compound **4** gives a *m*/*z* 162 ion that undergoes C_2D_3HN and C_2H_3N losses to produce *m*/*z* 117 and 121 ions, respectively. Reference compound **5** gives a *m*/*z* 162 ion that is unable to lose C_2H_3N and does not produce an abundant *m*/*z* 121 ion. The inability to lose C_2H_3N neutrals is indicative of C_6H_5 attachment to the nitrogen-3 position of the imidazole ring. Because the benzene *N*-(trideuteriomethyl)imidazole [adduct − H]$^+$ ion does not produce appreciable amounts of the *m*/*z* 121 ion, we propose that the adduct structure has a C_6H_5 moiety attached to the nitrogen-3 atom of the imidazole ring. Further proof of adduct structure could come from the study of an electron-ionized reference compound that is modeled after the putative adduct. We now know, however, that the adduct is a distonic ion, and its neutral counterpart is zwitterionic and impossible to synthesize. On the basis of the experimental results presented here, we now propose a reaction mechanism for the production of *N*-methylimidazole−benzene adduct ions in the gas phase (see eq 3).

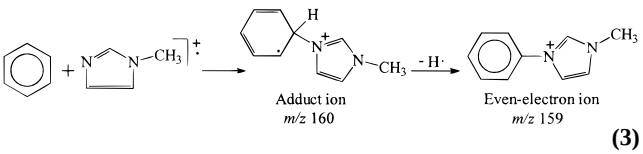

(3)

The data indicate that the hydrogen atom that is lost from the adduct is principally from the benzene moiety. Evidence for this is revealed by comparing the tandem mass spectrum of the *m*/*z* 160 adduct and of the *m*/*z* 159 [adduct − H]$^+$ ion (see Figures 2 and 4). A shift in product ions of *m*/*z* 78 (C_6H_6) to *m*/*z* 77 (C_6H_5) is observed. To test this proposal, benzene-d_6 was reacted with *N*-methylimidazole to form an adduct ion at *m*/*z* 166. The precursor ion was selected with a mass resolving power of 26 000 to isolate it from possible interference ions, and its CAD spectrum obtained. The spectrum in Figure 6 shows that predominantly deuterium atom loss occurs, supporting hydrogen atom loss from the benzene moiety as shown in eq 3. The fact that a less abundant hydrogen atom loss occurs suggests the adduct may be a mixture of two different loss mechanisms that yield the same product. If two loss mechanisms exist, Figure 6 shows that the deuterium atom loss is favored by approximately two to one; however, the extent of the loss of D gives a minimum estimate because there is likely a kinetic isotope effect.

Adduct Structure of the Naphthalene System. Because our ultimate goal is to determine the reactivity of gas-phase PAH radical cations, we chose to move from benzene to naphthalene. Recall from eq 2, the reaction pathway for this system involves the naphthalene radical cation reacting with an *N*-methylimidazole neutral to form a *m*/*z* 210 adduct. The first effort to investigate structure was to collect metastable and CAD spectra of the *m*/*z* 210 ion. The principal product ion is of *m*/*z* 128 (presumably the $C_{10}H_8$ naphthalene radical cation). Upon collisional activation, ions of *m*/*z* 128 and 209, the latter which is a result of hydrogen-atom loss, are produced. This adduct behaves similarly to that produced in the benzene reaction; that is, it fragments to give loss of H$^\bullet$ and to produce the aromatic hydrocarbon radical cation. These results suggest the naphthalene adduct structure is analogous to that of the

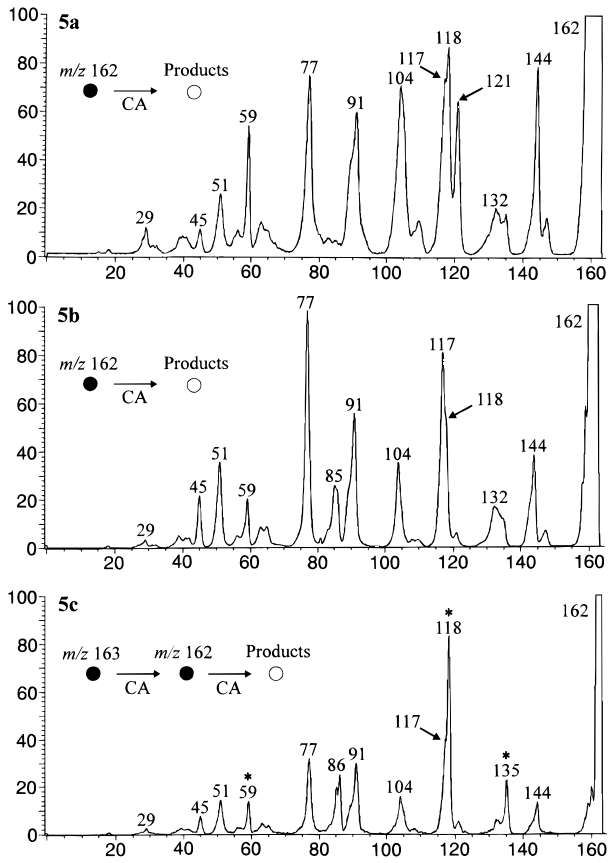

Figure 5. CAD spectrum of (a) [M + H]$^+$ of **4**, (b) preformed cation of **5**, and (c) [adduct − H]$^+$ from benzene and *N*-(trideuteriomethyl)-imidazole. An asterisk denotes metastable peaks which should not be used for comparison.

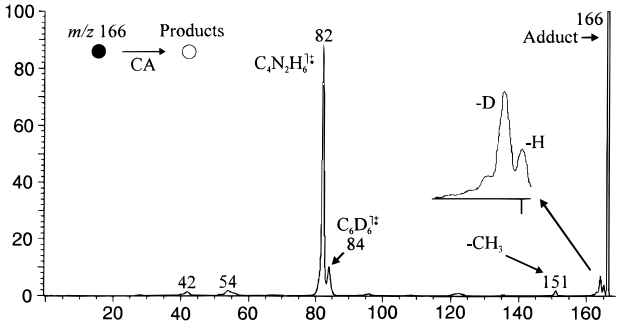

Figure 6. CAD spectrum of *m*/*z* 166 adduct produced in a mixture of ionized benzene-d_6 and *N*-methylimidazole.

benzene adduct; both involve covalent bonding of the hydrocarbon moiety to the imidazole ring.

To investigate further the structure of the naphthalene/*N*-methylimidazole adduct, the structure of the *m*/*z* 209 ion resulting from hydrogen atom loss from the adduct was probed through MS/MS/MS experiments. Analogous to the benzene system, the *m*/*z* 210 adduct ion is collisionally activated to produce [adduct − H]$^+$ ions, which were investigated in terms of their metastable-ion or collisionally activated decompositions. The *m*/*z* 209 ion undergoes metastable losses of 15, 27, and 41 u to form the ions of *m*/*z* 194, 182, and 168, respectively. The neutrals lost are identical in mass and the product ions are similar in relative abundance to those produced from the [adduct − H]$^+$ ion of the benzene system. CAD spectra of the *m*/*z* 209 ion show that, in addition to the metastable losses, and abundant *m*/*z* 127 ion ($C_{10}H_7$) and other ions are produced by cycloreversions of the imidazole and naphthalene rings. These

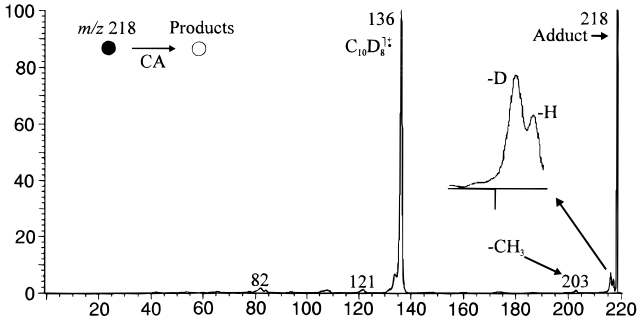

Figure 7. CAD spectrum of *m*/*z* 218 adduct produced in a mixture of ionized naphthalene-d_8 and *N*-methylimidazole.

fragmentations are consistent with those of the benzene adduct and its product formed by loss of H•, suggesting that the covalent attachment of the naphthalene moiety is to the N-3 atom of the imidazole ring.

Reference compounds for various naphthylimidazoles are more difficult to obtain, but the information acquired from the phenylimidazole standards is applicable to the naphthalene system. Phenyl attachment to the carbon-4 position of the imidazole ring results in CA-produced C_8H_6 ions whereas carbon-2 or nitrogen-3 attachments show C_7H_6N ions upon CA. The analogous attachments for the naphthalene system would produce adducts that fragment to $C_{12}H_8$ and $C_{11}H_8N$ ions of *m*/*z* 152 and 154, respectively. The lack of an abundant *m*/*z* 152 ion suggests the naphthalene moiety is attached to the carbon-2 or nitrogen-3 atom of the imidazole ring. Labeling experiments showed benzene attack at the C-2 position of *N*-(trideuteriomethyl)imidazole produces an adduct that loses 45 u (C_2D_3HN) and 41 mass units (C_2H_3N), whereas hydrocarbon attachment to the nitrogen-3 position gives an adduct that undergoes a dominant loss of 45. This information can be used as a signature for N-3 or C-2 attachment. To exploit this, naphthalene and *N*-(trideuteriomethyl)imidazole were ionized and allowed to react in the high-pressure region of a CI source to form an adduct of *m*/*z* 213. This ion was investigated by MS/MS/MS to determine whether losses of 41 and or 45 u occur from the CAD-produced *m*/*z* 212 ion. Only a loss of 45 is observed, suggesting attachment of the naphthalene moiety to the N-3 position of the imidazole ring. For benzene, all of the carbon atoms of the C_6H_6 ring are equivalent in reactivity but for naphthalene there are two reactive positions, C_1 (α) and C_2 (β). It was not determined which or if both positions are involved in the covalent binding of naphthalene to the nitrogen-3 position of the imidazole ring.

Analogous to the benzene system, we can ask whether the hydrogen atom loss is going from an adduct of *m*/*z* 210 to the fragment of *m*/*z* 209 is from the naphthalene moiety. Naphthalene-d_8 was reacted with *N*-methylimidazole in the high-pressure region of the tandem sector mass spectrometer. Figure 7 shows that, as in the benzene system, deuterium atom loss is favored versus hydrogen atom loss by a factor of 2 to 1. Although alternative pathways cannot be ruled out, eq 4 illustrates the predominate pathway for the formation of naphthalene/*N*-methylimidazole adducts.

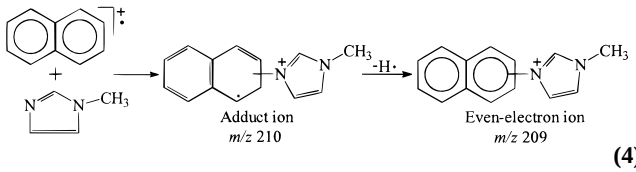

(4)

Conclusions

One goal of this work is to compare the gas-phase reactivity of benzene and naphthalene radical cations with a common nucleophile. Both systems produce radical cation adducts, but the PAH must have a lower IE than that of the nucleophile in order to observe adduct formation with a model biological nucleophile. After establishing the reactants for both systems, adducts were shown to form through predominant covalent attachment of the hydrocarbon to the nitrogen-3 atom of the imidazole ring. This conclusion was possible only after isotopic labeling of the methyl carbon, a result which can be applied to further systems.

A second goal is to establish a feasible protocol for studying the inherent gas-phase reactivity of a series of PAHs with a model biological nucleophile. The results of this study are a foundation for studies of higher mass PAH systems. Because *N*-methylimidazole reacts as a neutral with the naphthalene radical cation, the approach should be effectively applied to larger PAH systems. PAH radical cations react with DNA to give covalent attachment of the PAH to the nitrogen-7 position of adenine and guanine. The fact that similar attachments are found in these systems suggests that the gas-phase reactivity between a PAH radical cation and a model biological nucleophile correlate with biological activity. Future work will include both carcinogenic and noncarcinogenic PAHs to determine if a correlation can be more firmly established.

Acknowledgment. This research was supported by the National Institutes of Health (Grant Nos. 1P01CA49210 and 2P41RR00954).

JA9523404